

On/Off Switching of Perylene Tetracarboxylic Bisimide Luminescence by Means of Substitution at the N-Position by Electron-Rich Mono-, Di-, and Trimethoxybenzenes

Lucia Flamigni,^{*,[a]} Barbara Ventura,^[a] Andrea Barbieri,^[a] Heinz Langhals,^{*,[b]} Fritz Wetzel,^[b] Kerstin Fuchs,^[b] and Andreas Walter^[b]

Abstract: A series of perylene tetracarboxylic bisimides, substituted at the N-position with methoxyphenyl groups, have been synthesized together with model compounds and their photo-physical properties have been investigated by means of steady-state and time-resolved spectroscopic techniques. The luminescence properties of the examined compounds vary remarkably with the substitution pattern, with

emission quantum yields ranging from 1 to 10^{-2} – 10^{-3} . The observed quenching of the luminescence is assigned to a photoinduced electron transfer (PET) from the electron-rich methoxybenzene unit to the perylene bisimide moiety.

Keywords: bisimides • charge separation • electron transfer • luminescence • supramolecular chemistry

The radical anion of perylene bisimide has been detected by transient-absorption spectroscopy. The results could satisfactorily be explained by taking into consideration the redox potentials of the partners and the electron-releasing ability of each methoxy group in relation to its position with respect to N. Quantum-chemical calculations were also performed.

Introduction

On/off switching of luminophore emission by photoinduced electron transfer (PET) is an extensively explored area of research that has produced copious data and promising applications in the fields of sensing^[1] and information processing at the molecular level.^[2] Perylene tetracarboxylic bisimides (PIs) are a class of efficient luminophores, very stable and easily processable, with intense absorption in the visible range of the light spectrum; they can easily be functionalized to provide a variety of spectroscopic features.^[3–5] PIs, like other aromatic bisimides, are liable to a facile reduction ($E_0 \approx -0.6$ V vs. SCE) that leads to the formation of a radi-

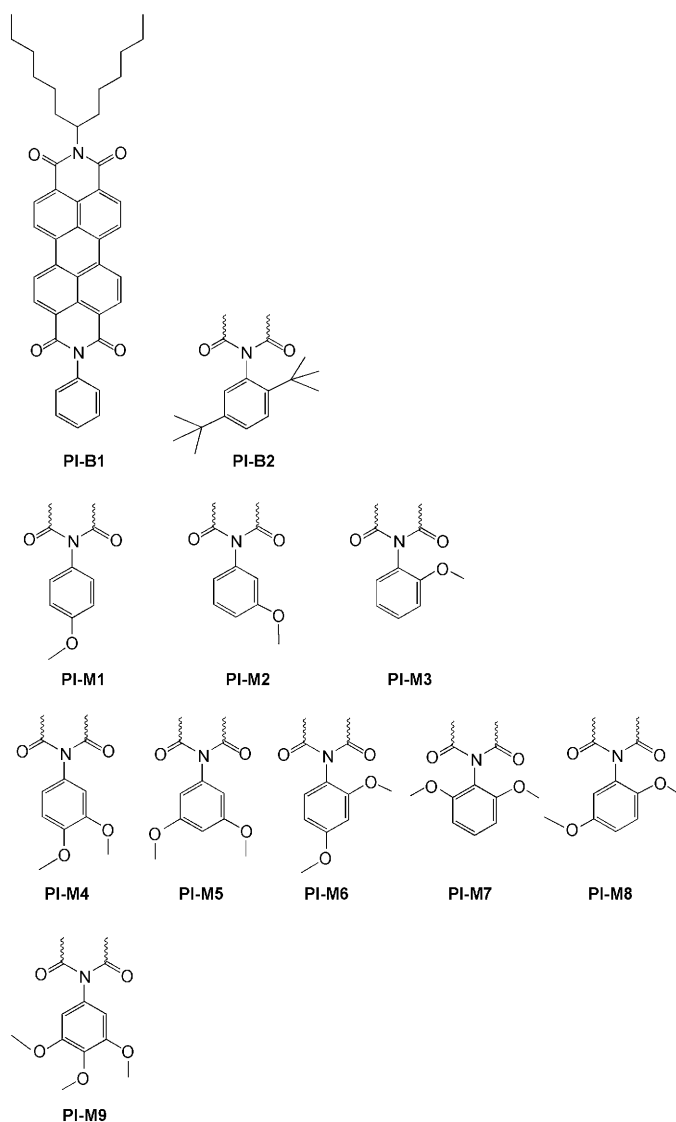
cal anion characterized by distinctive and intense absorption bands in the NIR region of the spectrum.^[6–8] This class of molecules is therefore well suited to mechanistic studies on electron-transfer processes. Excitation in the PI excited-state manifold (450–550 nm) leads to an excited state that has sufficient energy (around 2.3 eV) to accept in the semi-occupied HOMO an electron from the HOMO of a nearby electron-rich unit. Due to the short lifetime of the excited state (3.8 ns) the potential electron donor has to be very close, that is, it has to be either covalently or noncovalently connected to the PI unit to be able to interact. On the other hand, ground-state PIs can also accept in their LUMO electrons from the LUMO of excited chromophores, provided enough energy is stored in the donor excited state. In recent years we, as other groups, have extensively explored several molecular architectures of variable complexity, including PIs, with the aim of generating, upon an efficient HOMO–HOMO or LUMO–LUMO electron transfer, long-lived charge-separated (CS) states that might store light energy as electrochemical potential for useful reactions.^[8,9]

In the present report we focus on the mechanism of luminescence quenching by a series of similar electron-rich substituents, namely, mono-, di-, and trimethoxybenzenes, directly connected to the N-position of a PI (Scheme 1). The molecular design in this case has not been aimed toward

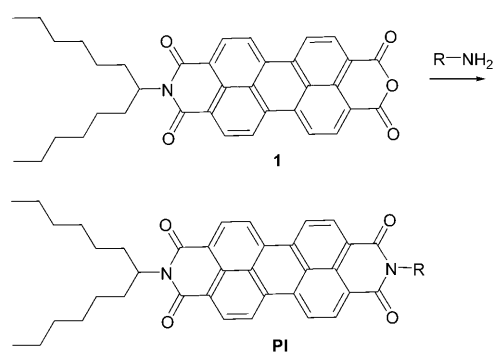
[a] Dr. L. Flamigni, Dr. B. Ventura, Dr. A. Barbieri
Istituto ISOF-CNR
Via P. Gobetti 101, 40129 Bologna (Italy)
Fax: (+39)051-639-9844
E-mail: flamigni@isof.cnr.it

[b] Prof. Dr. H. Langhals, Dr. F. Wetzel, Dr. K. Fuchs, A. Walter
Department of Chemistry, LMU University of Munich
Butenandtstrasse 13, 81377 Munich (Germany)
Fax: (+49)89-2180-77640
E-mail: Langhals@lrz.uni-muenchen.de

Supporting information for this article is available on the WWW under <http://dx.doi.org/10.1002/chem.201001489>.



Scheme 1. Molecular structures of the model compounds and substitution pattern at the N with related nomenclature.



Scheme 2. Synthesis of PI derivatives; for R see Scheme 1.

generating long-lived CS states, but rather to increase the electronic coupling between components. Therefore the electron-rich methoxy benzene groups have been directly

connected to the PI core. Different substitution patterns have been explored to understand the contribution of different parameters to the luminescence quenching of the PI luminophore. We will present the synthesis and the spectroscopic properties and the photophysical experiments designed to clarify the mechanism of on/off luminescence switching in the series of compounds and will discuss in detail the results also with the aid of molecular modeling.

Results and Discussion

Design and synthesis: The perylene derivatives were prepared in a one-step synthesis from the carboxylic anhydride^[10] **1** by condensation with primary amines in quinoline and imidazole,^[11] respectively, according to Scheme 2. Special care was taken in the chromatographic purification of the PI derivatives.

Absorption spectroscopy: The various compounds reported in Scheme 1 are an exhaustive series of mono-, di-, and trimethoxybenzene-substituted PI with reference models **PI-B1** and **PI-B2**. The former is a model that is missing the methoxy groups; the latter has been designed as model to test the steric effect of *ortho* substitution and separate it from the electronic effect induced by electron-rich methoxy derivatives at the same position. The compounds have been examined in low-polarity toluene (TL) and in medium-polarity dichloromethane (CH_2Cl_2), characterized by values of dielectric constant of around 2.4 and 8.9, respectively. This is useful in view of the expected effect of polarity on the possible charge-transfer reactions.

The absorption parameters in the two solvents are reported in the Supporting Information (Table S1), and a few examples of absorption spectra are reported in Figure 1 for solutions in TL and CH_2Cl_2 . The spectra of all compounds in TL are very similar, with band maxima at 526 or 527 nm and identical molar absorption coefficients within experimental errors. This is true also for CH_2Cl_2 solutions, in which the spectra display maxima shifted by 2 nm at 524 or 525 nm. The absence of, basically, any effect on the absorption spectra indicates that there are very little perturbations in the electronic properties of the PI core by the presence at the N-position of differently substituted methoxyphenyl groups. This has been observed before^[6,8] and is due to the fact that orbital nodes in the HOMO and LUMO at the N atom are present.^[12] Due to the decoupling between the PI core and the N-substituents, the present compounds can be regarded as assemblies made of two independent components, PI and methoxybenzene, and we will refer to them as dyads.

Luminescence spectroscopy: The luminescence properties of the series in the two solvents are collected in Table 1. The luminescence maxima in CH_2Cl_2 , at 530–532 nm, are hypsochromically shifted by 2–3 nm with respect to those in TL, at 532–534 nm, in agreement with the absorption spectra.

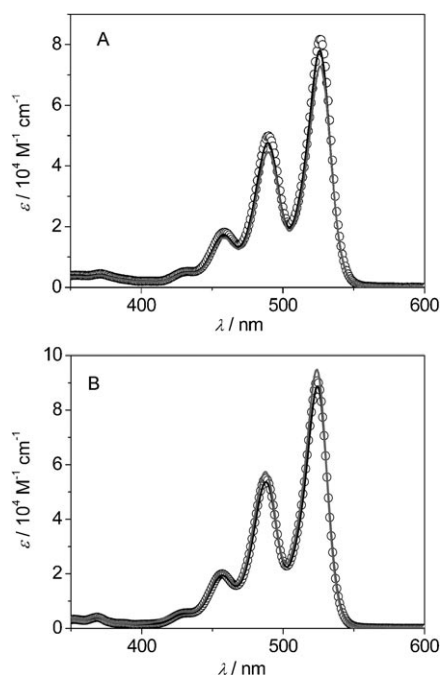


Figure 1. Absorption spectra: A) **PI-B1** (black line), **PI-M4** (gray line), and **PI-M9** (circles) in TL; B) **PI-B1** (black line), **PI-M3** (gray line), and **PI-M8** (circles) in CH_2Cl_2 .

Table 1. Luminescence data for the examined compounds in CH_2Cl_2 and TL. The quenched dyads are indicated in gray.

		295 K			77 K		
		λ_{max} [nm] ^[a]	Φ_{fl} ^[b]	τ [ns] ^[c]	λ_{max} [nm] ^[a]	τ [ns] ^[c]	E [eV] ^[d]
PI-B1	TL	532, 574, 622	0.98	3.8	542, 586, 637	3.8	2.29
	CH_2Cl_2	530, 572, 620	0.98	3.8			
PI-B2	TL	534, 576, 622	0.98	3.8	544, 588, 639	3.7	2.28
	CH_2Cl_2	530, 570, 620	0.99	3.7			
PI-M1	TL	534, 574, 620	0.19	0.720	543, 586, 637	3.8	2.28
	CH_2Cl_2	530, 572, 616	0.081	0.225			
PI-M2	TL	533, 574, 620	0.99	3.7	543, 586, 636	3.8	2.28
	CH_2Cl_2	530, 572, 618	0.72	2.6			
PI-M3	TL	533, 574, 620	0.98	3.9	543, 585, 637	3.8	2.28
	CH_2Cl_2	530, 571, 618	0.94	3.7			
PI-M4	TL	533, 574, 622	0.0069	0.010	543, 587, 637	3.4	2.28
	CH_2Cl_2	530, 572, 618	0.0067	0.010			
PI-M5	TL	533, 574, 622	0.20	0.840	543, 586, 637	3.7	2.28
	CH_2Cl_2	530, 570, 618	0.059	0.123			
PI-M6	TL	533, 574, 620	0.051	0.260	543, 585, 637	3.7	2.28
	CH_2Cl_2	530, 570, 616	0.016	0.046			
PI-M7	TL	533, 574, 620	0.99	3.9	542, 585, 636	3.8	2.29
	CH_2Cl_2	530, 570, 618	0.93	3.6			
PI-M8	TL	533, 574, 620	0.0036	ca. 0.005	543, 587, 638	3.2	2.28
	CH_2Cl_2	530, 571, 616	0.0030	ca. 0.005			
PI-M9	TL	534, 574, 624	0.013	0.033	541, 585, 637	3.5	2.29
	CH_2Cl_2	532, 572, 620	0.016	0.052			

[a] Data from uncorrected spectra. [b] Excitation at 490 nm in toluene and 489 nm in dichloromethane. For details, see the Experimental Section. [c] Excitation at 465 nm for nanosecond and at 532 nm for picosecond determinations. [d] From spectra recorded at 77 K.

Excitation spectra registered on the emission maxima perfectly match the absorption spectra, thereby indicating a genuine emission of the lowest singlet excited state. The luminescence quantum yield has values ranging from 0.99 to

10^{-2} – 10^{-3} , thereby indicating an extremely efficient quenching for some substitution patterns. The same substituent induces higher quenching in CH_2Cl_2 compared to TL (the case of **PI-M2**, unquenched in TL and slightly quenched in CH_2Cl_2 is emblematic), with the exception of the weakest emitters ($\phi_{\text{fl}} \leq 10^{-2}$), for which the emission yields in the two solvents are essentially the same within experimental errors (see Figure 2 for some selected cases). The fluorescence decays can be described by a single exponential in all cases, with values of lifetimes varying from (3.8 ± 0.1) ns for the unquenched dyads and the models to approximately 5 ps, which is the limit of the experimental resolution for emission experiments (Table 1). For both solvents, the decrease in lifetime parallels reasonably well the luminescence quantum yield, so that a radiative rate constant k_r ($k_r = \phi_{\text{fl}}/\tau$) on the order of $3\text{--}6 \times 10^8 \text{ s}^{-1}$ can be calculated for all dyads. This is a further indication that the PI intrinsic parameters are very little affected by the methoxy substitution, and that the donor and acceptor units are decoupled from an electronic viewpoint. Nonetheless, the presence of methoxy derivatives, in particular of the di- and trimethoxybenzenes with a substituent in the *para* position with respect to the N-linkage, leads to a strong quenching of the luminescence.

Quite remarkably, the fluorescence quenching is almost completely blocked in a rigid TL glass at 77 K for all systems except **PI-M4**, **PI-M8**, and **PI-M9**, which display slightly quenched lifetimes of 3.4, 3.2, and 3.5 ns, respectively, relative to the model lifetime of (3.8 ± 0.1) ns. These dyads also exhibit the highest fluorescence quenching at room temperature. For these, a low quenching rate on the order of 10^7 s^{-1} can be calculated at 77 K by the equation $k_q = 1/\tau - 1/\tau_0$, in which τ and τ_0 represent the lifetime of the excited state in the dyad and in the model **PI-B1**, respectively. As a general comment, we can certainly state that the process responsible for the luminescence quenching is thermally activated and disfavored in a rigid medium.

Time-resolved absorption: Further experiments were conducted by transient-absorption methods to detect possible non-luminescent reaction intermediates. Picosecond time-resolved

absorption spectra of optically matched solutions with excitation at 532 nm in the two solvents were performed. The spectra for selected cases are reported in Figure 3 and Figure 4 in TL and CH_2Cl_2 , respectively, and the data are

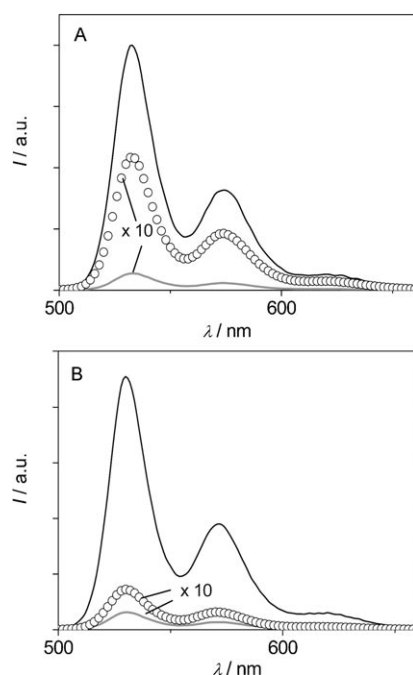


Figure 2. Uncorrected emission spectra: A) **PI-B1** (black line), **PI-M4** (gray line), and **PI-M6** (circles) in TL; B) **PI-B1** (black line), **PI-M4** (gray line), and **PI-M6** (circles) in CH_2Cl_2 .

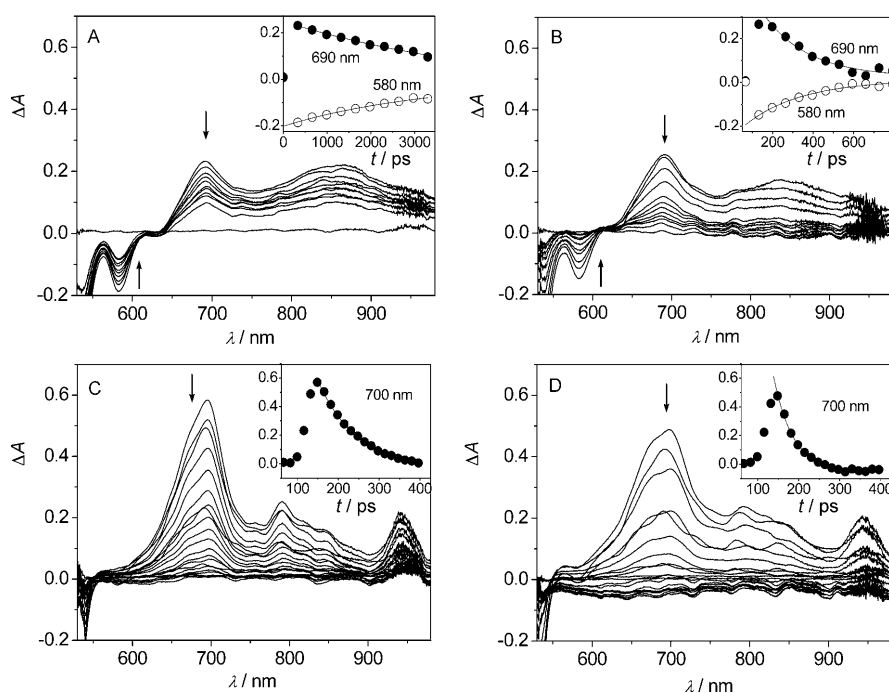


Figure 3. Time evolution of the absorption spectra registered after excitation with a laser pulse (35 ps, 532 nm, 3.5 mJ) of optically matched ($A=0.65$) solutions of A) **PI-B1**, B) **PI-M6**, C) **PI-M8**, and D) **PI-M4** in TL. For time delays of the spectra, see the insets in which time profiles at selected wavelengths and exponential fittings are displayed.

collected in Table 2. Model **PI-B1** displays different end of pulse absorption spectra in TL and CH_2Cl_2 (Figure 3A and 4A). In TL, negative signals around 580 and 620 nm, due to

the lowest energy bands of the stimulated emission, and positive peaks at 690 and around 850 nm are detected. In CH_2Cl_2 , the stimulated luminescence bands in **PI-B1** appears at around 575 and 620 nm, and a positive intense and sharp peak is found at 710 nm with a broad, lower structureless absorption that extends from 750 to 950 nm. Though different, the spectra were formerly identified as being due to the same species, the singlet excited state of PI chromophores, ^1PI .^[6] In agreement with this, they evolve very slowly on the explored timescale (0–3.3 ns) with a lifetime on the order of some nanoseconds, compatible with (3.8 ± 0.1) ns, the one derived from luminescence determinations. A more precise determination is precluded by the too-narrow time window explored during the experiment. The same spectral shape and time profile as **PI-B1** is displayed by solutions of the unquenched dyads **PI-B2**, **PI-M2**, **PI-M3**, and **PI-M7** in TL (spectra not shown); see Table 1. Likewise, the partially quenched dyads **PI-M1**, **PI-M5**, and **PI-M6** (see Figure 3B) display the same spectral shape as ^1PI and the decay lifetime is coincident, within experimental error, with that determined by luminescence (compare Table 1 with Table 2). On the contrary, the spectral shape displayed by the most-quenched dyads **PI-M4**, **PI-M8**, and **PI-M9**, characterized by a luminescence lifetime ≤ 30 ps, is different from that of ^1PI . The spectra do not have any stimulated

emission band but only positive absorptions at 700, 800, and 950 nm (Figure 3C and D). These spectral features are in reasonably good agreement with the anion radical PI^- in TL, with bands at 710, 800, and 960 nm.^[6,8a,9] This is an indication that the observed species is the reduced radical PI^- and, to further support this, the measured lifetimes of the absorbing species, 95 ps for **PI-M8**, 48 ps for **PI-M4**, and 50 ps for **PI-M9**, are different from those of ^1PI detected by luminescence techniques, around 5, 10, and 33 ps, respectively.

In CH_2Cl_2 , the detected species is that of the excited state ^1PI in all cases except **PI-M8** and, to some extent, **PI-M4** (Figure 4), as confirmed by the spectral shape. The time evolution of the absorbing intermediate is coincident with the luminescence lifetime, compare Table 1 with Table 2, except for **PI-M8** (Figure 4C) and **PI-M4**

(Figure 4D), for which the decay lifetimes measured at 710 nm are 30 and 20 ps, respectively. It is evident that in **PI-M8** the species formed and decaying within the pulse is

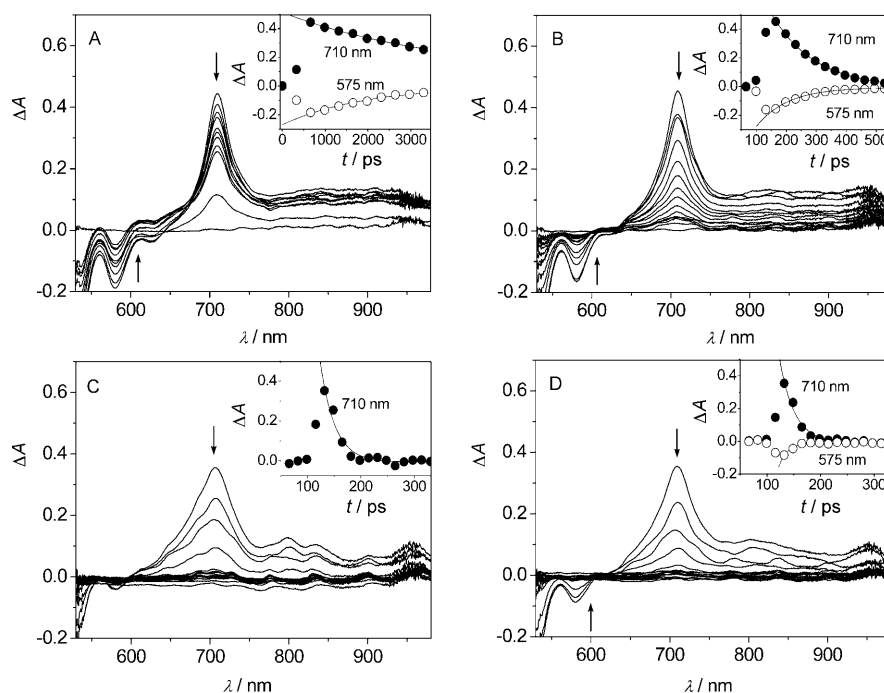


Figure 4. Time evolution of the absorption spectra registered after excitation with a laser pulse (35 ps, 532 nm, 3.5 mJ) of optically matched ($A=0.65$) solutions of A) **PI-B1**, B) **PI-M5**, C) **PI-M8**, and D) **PI-M4** in CH_2Cl_2 . For time delays of the spectra, see the insets in which time profiles at selected wavelengths and exponential fittings are displayed.

Table 2. Transient-absorption parameters and assignment of the bands for the examined compounds in CH_2Cl_2 and TL at 295 K. The quenched dyads are indicated in gray. In the last columns, the oxidation potential and the Hammett constant (σ) of the pertinent methoxybenzene are collected.

		295 K			Substituents	
Species		λ_{max} [nm] ^[a]	τ [ns] ^[b]	Oxidation potential (V vs. SCE)	$\sigma^{\text{[c]}}$	
PI-B1	TL	¹ PI	580 (bleaching), 690, 850	ca. 4.0	+2.48 ^[d]	
	CH_2Cl_2	¹ PI	575 (bleaching), 710	ca. 3.8		
PI-B2	TL	¹ PI	580 (bleaching), 690, 850	ca. 3.9	+2.06 ^[d]	-0.10
	CH_2Cl_2	¹ PI	575 (bleaching), 710	ca. 3.6		
PI-M1	TL	¹ PI	580 (bleaching), 690, 850	0.670	+1.76 ^[e]	-0.27
	CH_2Cl_2	¹ PI	575 (bleaching), 710	0.220		
PI-M2	TL	¹ PI	580 (bleaching), 690, 850	ca. 4.0	+1.76 ^[e]	0.12
	CH_2Cl_2	¹ PI	575 (bleaching), 710	ca. 2.5		
PI-M3	TL	¹ PI	580 (bleaching), 690, 850	ca. 3.7	+1.76 ^[e]	-
	CH_2Cl_2	¹ PI	575 (bleaching), 710	ca. 3.5		
PI-M4	TL	PI-	700, 800, 950	0.048	+1.45 ^[e]	0.12; -0.27
	CH_2Cl_2	¹ PI, PI-	575 (bleaching), 710, 850, 960	0.010, 0.020 ^[f]		
PI-M5	TL	¹ PI	580 (bleaching), 690, 850	0.810	+1.6 ^[g]	0.12; 0.12
	CH_2Cl_2	¹ PI	575 (bleaching), 710	0.130		
PI-M6	TL	¹ PI	580 (bleaching), 690, 850	0.250	+1.6 ^[g]	0.12; -0.27
	CH_2Cl_2	¹ PI	575 (bleaching), 710	0.060		
PI-M7	TL	¹ PI	580 (bleaching), 690, 850	ca. 4.0	+1.6 ^[g]	-; -
	CH_2Cl_2	¹ PI	575 (bleaching), 710	ca. 3.9		
PI-M8	TL	PI-	700, 800, 950	0.095	+1.34 ^[e]	-; 0.12
	CH_2Cl_2	PI-	710, 850, 960	0.030		
PI-M9	TL	PI-	700, 800, 950	0.050	+1.42 ^[e]	0.12; 0.12; -0.27
	CH_2Cl_2	¹ PI	575 (bleaching), 710	0.065		

[a] Detected band maxima, typical of the identified species. [b] The picosecond time-resolved experiment has a time window of 3.3 ns and allows the determination of lifetimes longer than 2 ns with rather low precision. [c] From ref. [15]. [d] E_{ox} in acetonitrile (vs. SCE) from ref. [13]. [e] $E_{1/2}$ in acetonitrile (vs. SCE) from ref. [14]. [f] See text for details. [g] Irreversible, calculated according to the equation in ref. [14].

the anion PI^- , with bands at 710, around 800, and 960 nm, and the absence of the stimulated emission bands at 575 nm. The situation is more ambiguous for **PI-M4** (see Figure 4D), in which a trace of stimulated emission at 575 nm with a very fast decay (on the order of 10 ps) can still be detected, but the spectrum has features that resemble those of the anion (see the band at 960 nm), and the measured lifetime at 710 nm is around 20 ps. In this case, we have clearly a mixture of ¹PI and PI^- , though a better description of the system is precluded by the time resolution of the apparatus. In all the examined cases, the transient spectra recovers back to the baseline, thus indicating that no further intermediate product is formed after the decay of either the singlet excited state or the anion.

Photoinduced processes: The strong luminescence of PI can be quenched to a great extent by substitution at the nodal N-position by a series of methoxybenzenes. Not all substitution patterns are effective in quenching the fluorophore luminescence; by inspection of Table 1 and Scheme 1, it is evident that there are several parameters to consider. Both the number of methoxy substituents and the relative position of the substituents with respect to each other or with respect to the attachment point to the PI structure are critical in achieving quenching. We can rationalize the different substitution patterns of the methoxybenzenes and the position of the attachment point to the PI structure with respect to the $-\text{OCH}_3$ group(s) if we examine: 1) the oxidation potentials of each single methoxybenzene substituent, and 2) the Hammett constants (σ) that describe the electron-releasing (negative σ)

or electron-withdrawing (positive σ) properties of the methoxy group(s) in the different positions with respect to N, the attachment point. The literature oxidation potentials for each methoxy benzene (or benzene) derivative^[13,14] of the dyad and the Hammett constants^[15] of the group(s) contained in the substituted benzene at the N-position are reported in the last two columns of Table 2. It should be noticed that the Hammett constants for *ortho* substitution are liable to large errors because of the difficulty in sorting electronic from steric factors and are therefore not provided. However, we will see that the simple parameters reported in the last two columns of Table 2 are sufficient to discuss the results.

As demonstrated by the absorption characteristics and by the constancy in the ¹PI radiative rate constants of the examined dyads, the two component units interact very little both in the ground and in the excited states. Quenching, when effective, therefore has to be ascribed to a “dynamic” interaction between the PI unit and the methoxybenzene unit that can transfer electrons to the partially empty HOMO of the PI unit, as confirmed by the detection of the anion radical PI⁻. The mechanism of electron transfer is also supported by the fact that the reaction is prevented at 77 K in a glass. This is typical for electron-transfer processes; in fact, whereas fluid solvents can stabilize the ionic products of charge-transfer reactions by reorientation of the solvent molecules, frozen solvents cannot do so and this often prevents electron transfer from occurring because of the insufficient or even negative driving force for the reaction.^[16] The discussion of the reaction dynamics within this series of dyads can be done on the basis of a very simple energy-level diagram (Figure 5). In this we report the energy levels of the PI chromophore at approximately 2.3 eV (¹PI) and at approximately 1.2 eV (³PI)^[17]; those are in fact the only excited states that can come into play upon excitation in the energy range above 350–400 nm. A relative scale of the energy levels of the charge-separated (CS) states formed upon HOMO–HOMO electron transfer from the methoxy derivative to the PI unit can be roughly estimated from an $E^{\circ} = -0.62$ V versus SCE in CH₂Cl₂ for PI^[6] and from the oxidation potentials of the substituents reported in Table 2. This allows one to derive approximate energy levels of the CS states that involve reduction of PI and oxidation of methoxybenzene (M), PI⁻-M⁺, at an energy ≥ 2.7 eV for **PI-B1** and **PI-B2**; at around 2.3 eV for the monosubstituted **PI-M1**, **PI-M2**, and **PI-M3**; at around 2.2 eV for the 1,3-derivatives **PI-M5**, **PI-M6**, and **PI-M7**; at around 2.1 eV for **PI-M4** and **PI-M9**; and below 2.0 eV for **PI-M8**.^[18] However, it is quite evident that the ability of the methoxy group(s) to release electrons is also important in the stabilization or destabilization of the methoxybenzene cation, which is formed upon electron transfer and, as such, the whole CS state. A higher stabilization of the CS state means a higher driving force for electron transfer and, as a consequence, a higher quenching rate. So, whereas monosubstituted methoxybenzenes with *ortho* or *meta* substitution (**PI-M2** and **PI-M3**) are not quenched, **PI-M1**, the one

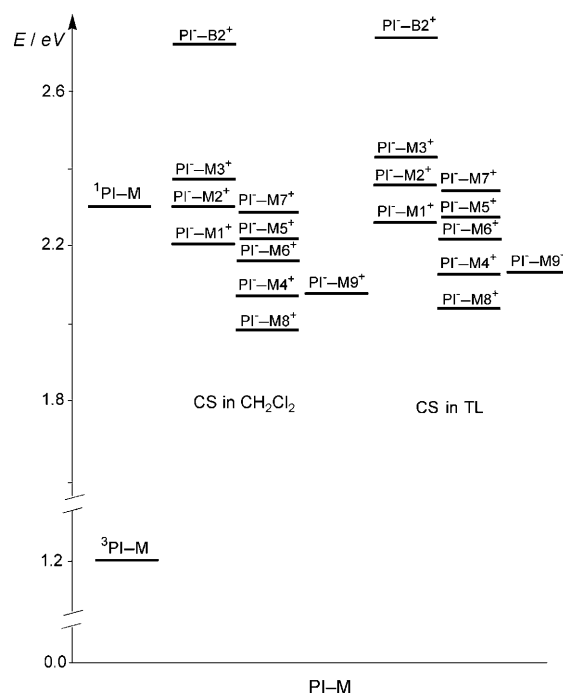


Figure 5. Schematic representation of the energy-level diagram for the examined dyads in CH₂Cl₂ and TL.

with an -OCH₃ group in the *para* position (negative σ), has a lower, more stabilized CS state and is quenched by electron transfer. A similar trend can be seen for the dimethoxy-substituted dyads, for which those with at least one *para* substituent with respect to N are more strongly quenched within the 1,2- and 1,3-substituted dyads. **PI-M8**, on the other hand, has no *para* substituent, but the 1,4-derivative can be oxidized more easily than all others (1.34 V vs. SCE). It is worth noting that **PI-M7** is not as liable to electron transfer as the other 1,3-derivatives, very likely because the two -OCH₃ groups *ortho* to N are less electron-releasing than the same groups *meta* to N. In the specific case of **PI-M7**, the assignment of the energy level of the CS state is based on kinetic evidence rather than on available data. Finally the trisubstituted 1,2,3-methoxy derivative, **PI-M9**, in spite of a slightly easier oxidation than the 1,2-methoxy derivative **PI-M4**, has an extra *meta* substituent that apparently slightly destabilizes the CS state, as demonstrated by the lower quenching. As is well known for electron-transfer reactions, a solvent polarity effect can also be noticed. This essentially leads to the stabilization of CS states in more polar CH₂Cl₂ (compared to TL), thus leading to a larger driving force for electron transfer and to a faster quenching. This trend can be clearly observed in dyads **PI-M1**, **PI-M2**, **PI-M5**, and **PI-M6**. The positive effect of higher polarity on the quenching levels off for more exoergonic reactions that are in the “activationless” region, according to Marcus theory.^[19] This is the case for **PI-M8**, **PI-M4**, and **PI-M9**.

In conclusion, a HOMO–HOMO electron transfer from a methoxybenzene unit to the excited PI unit can satisfactorily explain all experimental observations. Spectroscopic signa-

tures that indicate the presence of the radical anion PI^- have been distinguished in some cases. The detected spectrum should actually be due to the CS state $\text{PI}^- - \text{M}^+$, but for M^+ spectral features at $\lambda < 600$ nm and molar-absorbance coefficients on the order of $10^4 \text{ M}^{-1} \text{ s}^{-1}$ have been reported.^[20] This is an order of magnitude lower than the molar-absorption coefficient of PI^- ,^[21] so most probably the $\text{PI}^- - \text{M}^+$ spectral features in the examined spectral range resemble those of PI^- very closely. As stressed above, the CS-state spectral features are only detected in a few cases, namely, **PI-M8** and **PI-M4** in both solvents and **PI-M9** in TL only, and these are also the cases characterized by faster luminescence quenching, that is, by a fast rate of charge separation. This can be easily understood if we consider the following consecutive kinetic scheme for the generic dyad PI-M .



In the presence of a fast charge recombination (CR), the species $\text{PI}^- - \text{M}^+$ cannot accumulate when the rate of charge separation (CS) is rather low and therefore cannot be detected. Only when CS is extremely fast, or at least faster than CR, does the species build up to the point where it can be detected and its lifetime measured. This is the case of $\text{PI}^- - \text{M}^+$ in **PI-M8**, **PI-M4**, and **PI-M9** in TL, which have CR lifetimes of 95, 48, and 50 ps compared to CS lifetimes of approximately 5, 10, and 33 ps, respectively. This is also true for **PI-M8** in CH_2Cl_2 , which has a CR lifetime of 30 ps, compared to a CS lifetime of around 5 ps. More ambiguous is the case of **PI-M4** in CH_2Cl_2 (see Figure 4D), for which CS and CR rates are closer than in the other cases—10 and 20 ps, respectively—and the detected product is a mixture of ${}^1\text{PI-M}$ and $\text{PI}^- - \text{M}^+$ that evolves and decays within the pulse length. As far as the CR rate is concerned, from the few data available, the effect of the Marcus inverted region is evident.^[19] In fact, in CH_2Cl_2 , in which the driving force for recombination is lower (i.e., a more stabilized CS state) and in which the polarity of the solvent enhances the reorganizational energy, recombination is faster than in TL (Table 2). In spite of the presence of a low-lying triplet excited state at 1.2 eV, ${}^3\text{PI-MB}$, recombination of $\text{PI}^- - \text{M}^+$ occurs to the singlet ground state, as testified by the baseline recovery of the transient absorption spectrum. PI triplet is also known to have, in addition to features around 500 nm, bands in the NIR and should be detected in the present experiments, if formed.^[17,22]

Molecular modeling: The results of the complex spectroscopic behavior may be confirmed by means of quantum-chemical calculations. We applied the DFT B3-LYP method and simplified the structure of **PI-M1–PI-M9** by means of the replacement of the 1-hexylheptyl alkyl group by the electronically similar methyl group to obtain **PI-M1'–PI-M9'**. The calculations indicate energetically high-lying occupied orbitals centered on the methoxyphenyl substituent with energies close to the HOMO of the PI chromophore. Slight structural variations can control the energetic position

of these orbitals. Fluorescence remains unaffected by these substituents if their occupied orbitals are below the HOMO of the chromophore that represents type I in Figure 6, such

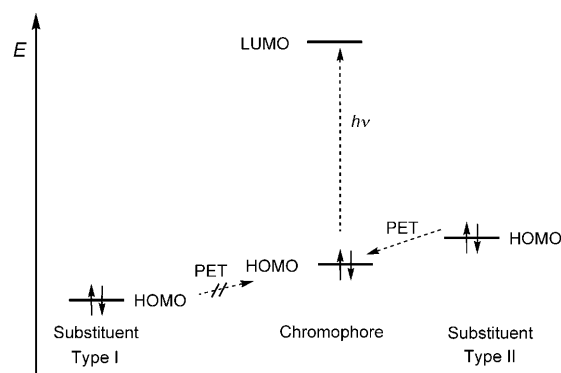


Figure 6. Electronic terms of PI-M . Left: Electron-depleted substituent (type I); right: electron-rich substituent (type II).

as for the simple phenyl derivatives **PI-B1** and **PI-B2**, and even for the methoxy derivative **PI-M3'** whose the orbitals are shown in Figure 7. Moreover, two methoxy groups in the *ortho* positions are not sufficient to interconvert the position of the orbitals (**PI-M7'**). As a consequence, no photo-induced electron transfer (PET) can proceed and perturb fluorescence so that unaltered high-fluorescence quantum yields were found. This situation changes completely for the trimethoxy derivative **PI-M9'** in which two occupied orbitals of the substituent are energetically above the HOMO of the PI chromophore (see the right side of Figure 6, type II, and the right side of Figure 7). As a consequence, an electronic excitation ($h\nu$ in Figure 6) leaves the HOMO of the chromo-

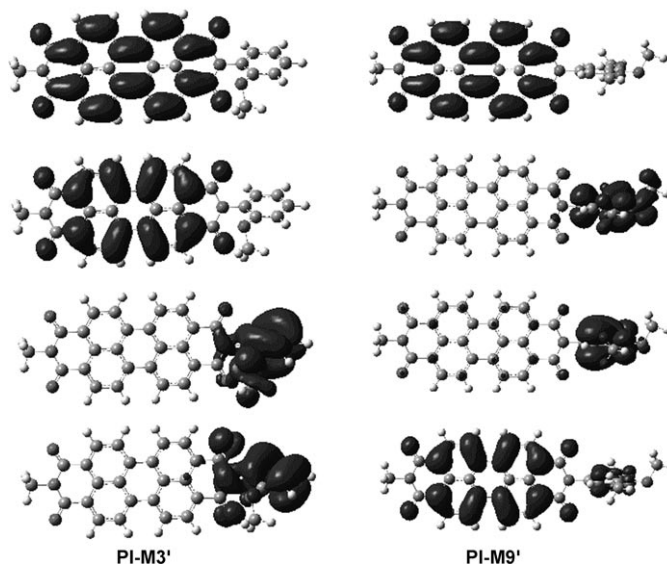


Figure 7. Orbitals of the methyl analogues of PI-M ($\text{PI-M}'$). From bottom to top (DFT B3-LYP): HOMO-2, HOMO-1, HOMO, LUMO. From left to right: **PI-M3'** and **PI-M9'**.

phore semioccupied and a PET proceeds from the type II side chain to the chromophore, fills the vacant position, and inhibits fluorescence by this competition. One methoxy group in the 4-position of the phenyl group to form **PI-M1'** is sufficient to lift one filled orbital above the HOMO of the chromophore and to dampen the fluorescence quantum yield to 8% in CH₂Cl₂. The spectroscopic behavior becomes more complex for **PI-M2** in which both the filled orbitals of the chromophore and of the methoxyphenyl substituent are energetically similar and external influences, such as solvent polarity, may switch from type I to type II and thus switch fluorescence quantum yield.

The calculated structures concern the gas phase and all effects can be modulated by solvents. Thus, the comparably high influence of the solvent polarity on the efficiency of PET becomes understandable.

Conclusion

The effect of a series of electron-rich substituents directly connected to the N-position of perylene tetracarboxylic bisimide derivatives on the switching from a strong fluorescence to an efficient generation of charge-separated excited states by photoinduced electron transfer (PET) has been examined. The spectroscopic results have been rationalized in terms of 1) the oxidation potentials of each single methoxybenzene substituent, 2) the Hammett constants of the methoxy groups, and 3) quantum chemical calculations.

The absorption spectra, very similar for all examined compounds and with identical absorption coefficients, indicate very little perturbations in the electronic properties of the PI core by the presence at the N-position of differently substituted methoxyphenyls, due to the presence of orbital nodes at the N atom. In accordance, luminescence maxima are the same for all compounds and are only slightly affected by the solvent polarity. On the other hand, the luminescence quantum yields range from approximately 1 to 10⁻²–10⁻³, thereby indicating an extremely efficient quenching for some substitution patterns (in particular for the case of di- and trimethoxybenzenes when a substituent in the *para* position with respect to the N linkage is present). Transient-absorption experiments have allowed the detection of the short-lived PI anion radical, thus indicating the population of a charge-separated state, which was not the case for the emitting derivatives. In all the examined cases, no further intermediate is formed after the decay of either the singlet excited state or the anion. A HOMO–HOMO electron transfer from the methoxybenzene unit to the excited PI unit can satisfactorily explain all experimental observations. The analysis of the spectroscopic results has been confirmed by quantum-mechanical calculations. In conclusion, the observed switching is driven by the energy of the methoxybenzene-occupied orbitals with respect to the energy of the perylene bisimide HOMO controlled by the positioning of the methoxy substituents and may be further fine-tuned by means of solvent effects.

Experimental Section

General: IR spectra were obtained using a Perkin–Elmer 1420 Ratio Recording Infrared Spectrometer, FT 1000. UV/Vis spectra were obtained using Varian Cary 5000 and Bruins Omega 20, and fluorescence spectra were obtained using a Varian Eclipse instrument. NMR spectroscopy was carried out using a Varian VNMRs 600 (600 MHz), and mass spectrometry was conducted using a Finnigan MAT 95 instrument.

Compound PI-B1: 9-(1-Hexylheptyl)-2-benzopyrano[6',5',4':10,5,6]anthra[2,1,9-*def*]isoquinoline-1,3,8,10-tetraone (2.00 g, 3.48 mmol), formamide (847 mg, 6.26 mmol), zinc acetate (100 mg, 0.45 mmol), and imidazole (10 g) under argon were heated at 180 °C for 10 h and then allowed to cool. While still warm, the solution was treated with 2N aqueous HCl (55 mL), then collected by vacuum filtration, dried at 120 °C in air (2.15 g, 95%), purified by column separation (silica gel, chloroform), evaporated, washed with distilled water, and dried under a medium vacuum (50 °C, 4 h). Yield: 1.40 g (62%); *R_f* (silica gel, CHCl₃) = 0.53; ¹H NMR (CDCl₃): δ = 0.81 (t, 6H; 2 × CH₃), 1.22 (m, 16H; 8 × CH₂), 1.87 (m, 2H; 1 × α-CH₂), 2.23 (m, 2H; 1 × α-CH₂), 5.17 (m, 1H; 1 × CH), 7.45 (m, 5H; phenyl), 8.6 ppm (m, 8H; perylene); ¹³C NMR (CDCl₃): δ = 14.03, 22.58, 26.95, 29.21, 31.76, 32.38, 54.85 (7 C-1-hexylheptyl), 123.03, 123.36, 123.31, 126.39, 126.65, 128.60, 128.88, 129.45, 129.53, 129.82, 131.77, 134.26, 135.08, 135.09 (14 × C_{aryl}), 163.53 ppm (C=O); IR (KBr): $\tilde{\nu}$ = 2955 (m), 2927 (m), 2857 (m), 1699 (s), 1660 (s), 1594 (s), 1579 (m), 1505 (w), 1490 (w), 1455 (w), 1433 (w), 1405 (m), 1334 (s), 1255 (m), 1199 (w), 1177 (m), 1124 (w), 1110 (w), 1075 (w), 965 (m), 852 (w), 840 (w), 810 (s), 745 (s), 700 (w), 637 cm⁻¹ (w); UV (CHCl₃): λ_{max} (ε) = 492 (18750), 492 (52270), 528 nm (86730 mol⁻¹ dm³ cm⁻¹); fluorescence (CHCl₃): λ_{max} = 538, 578 nm; MS (70 eV): *m/z* (%): 650 (5), 649 (23), 648 (47) [M⁺], 631 (7), 479 (4), 469 (3), 468 (18), 467 (60), 466 (100) [M⁺ - C₁₃H₂₆], 465 (18), 449 (5), 422 (6), 421 (8), 373 (3), 345 (1), 233 (1), 69 (2), 55 (4), 41 (2), 28 (1); elemental analysis calcd (%) for C₄₃H₄₀N₂O₄: C 79.60, H 6.21, N 4.31; found: C 79.61, H 6.28, N 4.49.

Compound PI-M3: 9-(1-Hexylheptyl)-2-benzopyrano[6',5',4':10,5,6]anthra[2,1,9-*def*]isoquinoline-1,3,8,10-tetraone (350 mg, 0.61 mmol), 2-anisidine (225 mg, 1.83 mmol), the amount of a microspatulum of zinc acetate dihydrate, and imidazole (5 g) were heated at 140 °C for 4 h. While still warm, the solution was treated with 2N aqueous HCl (30 mL), stirred at room temperature for 2 h, collected by vacuum filtration, washed with distilled water, dried in air at 120 °C, purified by column separation (silica gel, chloroform to remove a forerun and then chloroform/acetone 10:1), concentrated by vacuum distillation, precipitated with methanol, and dried in air at 120 °C. Yield: 210 mg (51%); m.p. > 250 °C; *R_f* (silica gel, CHCl₃/acetone 10:1) = 0.87; ¹H NMR (300 MHz, CDCl₃): δ = 0.83 (t, *J*(H,H) = 6.6 Hz, 6H; 2 × CH₃), 1.24–1.32 (m, 16H; 8 × CH₂), 1.84–1.92 (m, 2H; β-CH₂), 2.20–2.30 (m, 2H; β-CH₂), 3.81 (s, 3H; -OCH₃), 5.14–5.22 (m, 1H; α-CH), 7.10–7.52 (m, 4H; CH_{aryl}), 8.58–8.71 ppm (m, 8H; CH_{perylene}); ¹³C NMR (75 MHz, CDCl₃): δ = 14.1 (CH₃), 22.6 (CH₂), 27.0 (CH₂), 29.2 (CH₂), 31.8 (CH₂), 32.4 (CH₂), 45.8 (CH), 55.9 (-OCH₃), 112.1, 121.1, 123.0, 123.2, 123.5, 123.9, 126.4, 126.7, 129.6, 129.9, 130.0, 10.5, 131.1, 131.7, 134.4, 134.9, 155.0, 163.2, 164.6 ppm; IR (KBr): $\tilde{\nu}$ = 3433 (br w), 3072 (br vw), 2954 (m), 2927 (m), 2856 (m), 1928 (br vw), 1712 (s), 1698 (s), 1658 (vs), 1595 (s), 1579 (m), 1502 (m), 1465 (w), 1434 (m), 1404 (m), 1344 (vs), 1305 (w), 1281 (w), 1255 (s), 1198 (w), 1177 (m), 1139 (vw), 126 (w), 1109 (w), 1045 (w), 1027 (w), 965 (w), 847 (w), 774 (vw), 747 (m), 729 (m), 696 (vw), 634 (w), 607 (vw), 572 (vw), 532 (vw), 495 (w), 430 cm⁻¹ (w); UV/Vis (CHCl₃): λ_{max} (*E_{rel}*) = 526.0 (1.0), 489.0 (0.60), 458.2 nm (0.21); fluorescence (CHCl₃): λ_{max} = 534, 576 nm; fluorescence quantum yield (λ_{exc} = 489 nm, c = 5.8 × 10⁻⁶ mol L⁻¹ in chloroform, reference 2,9-bis-(1-hexylheptyl)anthra[2,1,9-*def*:6,5,10-*d'e'*]diisoquinoline-1,3,8,10-tetraone with Φ = 1.0): 1.0; MS (70 eV): *m/z* (%): 678 (93) [M⁺], 661 (12) [M⁺ - OH], 647 (3) [M⁺ - OMe], 593 (3), 523 (2), 497 (64) [M⁺ - C₁₃H₂₅], 479 (6) [479 - H₂O], 465 (100) [647 - C₁₃H₂₈], 437 (3) [465 - CO], 390 (9) [465 - C₆H₅]; elemental analysis calcd (%) for C₄₄H₄₂N₂O₅: C 77.85, H 6.24, N 4.13; found: C 77.70, H 6.13, N 4.10.

Compound PI-M1: 9-(1-Hexylheptyl)-2-benzopyrano[6',5',4':10,5,6]anthra[2,1,9-*def*]isoquinoline-1,3,8,10-tetraone (460 mg, 800 μmol), 4-anisidine (195 mg, 1.58 mmol), zinc acetate (37 mg, 0.20 mmol), and quinoline

(7 mL) were stirred at 210°C for 6 h under Ar atmosphere (dark red solution) and then allowed to cool. While still warm and with strong stirring, the solution was added dropwise to methanol/distilled water 1:1 (700 mL), stirred for 2 h, allowed to stand for 16 h, collected by vacuum filtration, washed with boiling distilled water (300 mL) and a mixture of distilled water and methanol (1:1, 300 mL), dried under vacuum at 90°C for 24 h, dissolved in the minimal amount of CHCl₃/MeOH=80:1, and purified by column separation (short column of neutral alumina, CHCl₃/MeOH=80:1, dark red first fraction). Yield: 504 mg (93%); m.p. >300°C; *R_f* (CHCl₃/MeOH=60:1): 0.4; *R_f* (silica gel, CHCl₃/acetone 10:1)=0.79; ¹H NMR (600 MHz, CDCl₃, 27°C, TMS): δ=8.73–8.62 (m, 8H; CH_{perylene}), 7.28 (d, ³J(H,H)=8.9 Hz, 2H; CH_{arom.}), 7.09 (d, ³J(H,H)=8.9 Hz, 2H; CH_{arom.}), 5.21–5.16 (m, 1H; CH), 3.89 (s, 3H; O-CH₃), 2.28–2.22 (m, 2H; CH₂), 1.91–1.85 (m, 2H; CH₂), 1.38–1.19 (m, 16H; 8×CH₂), 0.83 ppm (t, ³J(H,H)=7.1 Hz, 6H; CH₃); ¹³C NMR (150 MHz, CDCl₃, 27.0°C): δ=163.8, 159.7, 135.0, 134.3, 131.8, 131.1, 129.8, 129.5, 127.5, 126.6, 126.4, 123.4, 123.2, 123.0, 114.8, 55.5, 54.8, 32.4, 31.7, 29.2, 26.9, 22.6, 14.0 ppm; IR (ATR): $\tilde{\nu}$ =2954 (w), 2925 (m), 2856 (w), 1697 (s), 1655 (s), 1594 (s), 1577 (m), 1510 (s), 1484 (w), 1459 (w), 1434 (w), 1404 (m), 1342 (s), 1301 (m), 1249 (s), 1176 (m), 1145 (w), 1124 (w), 1107 (w), 1030 (m), 966 (m), 849 (m), 832 (m), 809 (s), 794 (s), 744 (s), 704 (w), 694 (w), 638 (w), 616 (w), 607 cm⁻¹ (w); UV/Vis (CHCl₃): λ_{max} (*E_{rel}*)=459.2 (0.22), 491.0 (0.60), 527.0 nm (1.00); fluorescence (CHCl₃): λ_{max} (*I*)=534.3 (1.00), 577.5 (0.52); fluorescence quantum yield: (CHCl₃, λ_{exc} =491 nm, *E_{491nm/1cm}*=0.01587, reference: 2,9-bis-(1-hexylheptyl)anthra[2,1,9-*def*:6,5,10-*d'ef'*]diisoquinoline-1,3,8,10-tetraone^[4] with $\Phi=1.0$): 0.08; MS (DEP/EI): *m/z* (%): 678 (51) [*M*⁺], 496 (100) [*M*⁺-C₁₃H₂₆]; HRMS: *m/z*: calcd for C₄₄H₄₂N₂O₅: 678.3094; found: 678.3098, $\Delta=0.0004$; elemental analysis calcd (%) for C₄₄H₄₂N₂O₅: C 77.85, H 6.24, N 4.13; found: C 77.80, H 6.17, N 4.13.

Compound PI-M2: 9-(1-Hexylheptyl)-2-benzopyrano[6',5',4':10,5,6]anthra[2,1,9-*def*]isoquinoline-1,3,8,10-tetraone (460 mg, 800 μmol), 3-anisidine (194 mg, 1.58 mmol), zinc acetate (30 mg, 0.16 mmol), and quinoline (7 mL) were allowed to react and the product was purified as was described for **PI-M1** (5 h, 210°C, dried at 90°C). Yield: 476 mg (88%); m.p. >300°C; *R_f* (CHCl₃/MeOH=60:1)=0.5; *R_f* (silica gel, CHCl₃/acetone 10:1)=0.78; ¹H NMR (600 MHz, CDCl₃, 27°C, TMS): δ=8.74–8.62 (m, 8H; CH_{perylene}), 7.51–7.47 (m, 1H; CH_{arom.}), 7.06 (ddd, ³J(H,H)=8.5 Hz, ⁴J(H,H)=2.5 Hz, ⁵J(H,H)=0.9 Hz, 1H; CH_{arom.}), 6.96–6.93 (m, 1H; CH_{arom.}), 6.91–6.90 (m, 1H; CH_{arom.}), 5.22–5.15 (m, 1H; CH), 3.85 (s, 3H; CH₃), 2.29–2.20 (m, 2H; CH₂), 1.91–1.83 (m, 2H; CH₂), 1.38–1.20 (m, 16H; 8×CH₂), 0.82 ppm (t, ³J(H,H)=6.9 Hz, 6H; CH₃); ¹³C NMR (150 MHz, CDCl₃, 27.0°C): δ=163.5, 160.5, 136.1, 135.1, 134.3, 131.8, 130.1, 129.8, 129.5, 126.7, 126.4, 123.3, 123.0, 120.7, 115.0, 114.2, 55.4, 54.8, 32.4, 31.7, 29.2, 26.9, 22.6, 14.0 ppm; IR (ATR): $\tilde{\nu}$ =2956 (w), 2924 (m), 2856 (w), 1696 (s), 1658 (s), 1594 (s), 1577 (m), 1506 (w), 1487 (w), 1456 (w), 1435 (w), 1404 (m), 1345 (s), 1320 (w), 1256 (s), 1214 (w), 1180 (m), 1125 (w), 1110 (w), 1035 (w), 966 (w), 858 (m), 810 (s), 796 (s), 778 (m), 764 (w), 744 (s), 704 (w), 686 (m), 638 (w), 609 cm⁻¹ (w); UV/Vis (CHCl₃): λ_{max} (*E_{rel}*)=458.8 (0.24), 490.0 (0.61), 527.0 nm (1.00); fluorescence (CHCl₃): λ_{max} (*I*)=534.5 (1.00), 577.5 (0.51); fluorescence quantum yield (CHCl₃, λ_{exc} =490 nm, *E_{490nm/1cm}*=0.01423, reference: 2,9-bis-(1-hexylheptyl)anthra[2,1,9-*def*:6,5,10-*d'ef'*]diisoquinoline-1,3,8,10-tetraone^[4] with $\Phi=1.0$): 0.77; MS (DEP/EI): *m/z* (%): 678 (51) [*M*⁺], 496 (100) [*M*⁺-C₁₃H₂₆]; HRMS: *m/z*: calcd for C₄₄H₄₂N₂O₅: 678.3094; found: 678.3097, $\Delta=0.0003$; elemental analysis calcd (%) for C₄₄H₄₂N₂O₅: C 77.85, H 6.24, N 4.13; found C 78.06, H 6.32, N 4.15.

Compound PI-M8: 9-(1-Hexylheptyl)-2-benzopyrano[6',5',4':10,5,6]anthra[2,1,9-*def*]isoquinoline-1,3,8,10-tetraone (172 mg, 0.30 mmol) and 2,5-dimethoxyaniline (230 mg, 1.50 mmol) were allowed to react and the product was purified as was described for **PI-M3**. Yield: 140 mg (66%); m.p. >250°C; *R_f* (silica gel, CHCl₃/acetone 10:1)=0.79; ¹H NMR (300 MHz, CDCl₃): δ=0.85 (t, *J*(H,H)=6.6 Hz, 6H; 2×CH₃), 1.26–1.35 (m, 16H; 8×CH₂), 1.85–1.92 (m, 2H; α-CH₂), 2.22–2.32 (m, 2H; α-CH₂), 3.78 (s; CH₃, -OCH₃), 3.83 (s, 3H; CH₃), 5.16–5.26 (m, 1H; -N-CH), 6.94–7.28 (m, 3H; CH_{aryl}), 8.60–8.74 ppm (m, 8H; CH_{perylene}); ¹³C NMR (75 MHz, CDCl₃): δ=14.4 (CH₃), 23.0 (CH₂), 27.3, (CH₂), 29.6 (CH₂), 32.2 (CH₂), 32.8 (CH₂), 55.2 (CH), 56.2 (-OCH₃), 56.8 (-OCH₃), 113.4, 116.0, 116.1, 123.4, 123.6, 123.9, 124.7, 126.8, 127.1, 129.9, 130.4, 131.5,

132.1, 135.3, 149.6, 154.2, 163.5, 163.9 ppm; IR (KBr): $\tilde{\nu}$ =3435 (brm), 3081 (brw), 2954 (m), 2927 (m), 2856 (m), 1711 (s), 1698 (s), 1659 (vs), 1618 (w), 1595 (s), 1579 (m), 1508 (s), 1466 (m), 1432 (m), 1405 (m), 1344 (vs), 1315 (m), 1275 (m), 1254 (s), 1232 (m), 1217 (m), 1198 (w), 1177 (m), 1148 (vw), 1127 (w), 1107 (w), 1042 (w), 966 (w), 854 (w), 810 (m), 777 (vw), 749 (m), 729 (vw), 648 (w), 608 (vw), 496 (w), 430 cm⁻¹ (w); UV/Vis (CHCl₃): λ_{max} (*E_{rel}*)=526.1 (1), 489.8 (0.58), 458.2 nm (0.21); fluorescence (CHCl₃): λ_{max} =533, 576 nm; fluorescence quantum yield (λ_{exc} =489 nm, *c*=1.0×10⁻⁶ mol L⁻¹ in chloroform, reference 2,9-bis-(1-hexylheptyl)anthra[2,1,9-*def*:6,5,10-*d'ef'*]diisoquinoline-1,3,8,10-tetraone^[4] with $\Phi=1.0$): 0.02; MS (70 eV): *m/z* (%): 708 (100) [*M*⁺], 691 (6) [*M*⁺-OH], 677 (16) [*M*⁺-OMe], 527 (34) [*M*⁺-C₁₃H₂₅], 495 (78) [677-C₁₃H₂₆], 390 (3) [495-C₆H₂OMe], 373 (8) [390-OH], 435 (3) [373-CO]; elemental analysis calcd (%) for C₄₅H₄₄N₂O₆: C 76.25, H 6.26, N 3.95; found C 76.41, H 6.23, N 3.91.

Compound PI-M6: 9-(1-Hexylheptyl)-2-benzopyrano[6',5',4':10,5,6]anthra[2,1,9-*def*]isoquinoline-1,3,8,10-tetraone (57 mg, 0.30 mmol) and 2,4-dimethoxyaniline (54 mg, 0.40 mmol) were allowed to react and the product was purified as was described for **PI-M3**. Yield: 45 mg (63%); m.p. >250°C; *R_f* (silica gel, CHCl₃/acetone 10:1)=0.76; ¹H NMR (300 MHz, CDCl₃): δ=0.76 (t, *J*(H,H)=6.6 Hz, 6H, 2×CH₃), 1.17–1.26 (m, 16H; 8×CH₂), 1.77–1.83 (m, 2H; α-CH₂), 2.10–2.24 (m, 2H; α-CH₂), 3.71 (s; CH₃, -OCH), 3.81 (s, 3H; OCH₃), 5.08–5.18 (m, 1H; -N-CH), 6.58–6.60 (m, 1H; CH_{aryl}), 7.13–7.19 (m, 2H; 2×CH_{aryl}), 8.52–8.65 ppm (m, 8H; CH_{perylene}); ¹³C NMR (75 MHz, CDCl₃): δ=4.4 (CH₃), 23.0 (CH₂), 27.4 (CH₂), 29.6 (CH₂), 32.2 (CH₂), 32.8 (CH₂), 55.2 (CH), 56.0, (-OCH₃), 100.2, 105.3, 117.1, 123.4, 123.6, 126.8, 127.1, 130.0, 130.6, 131.5, 132.1, 134.8, 135.3, 156.2, 161.8, 163.8 ppm; IR (KBr): $\tilde{\nu}$ =3435 (brw), 2926 (m), 2856 (m), 1698 (vs), 1594 (m), 1513 (m), 1465 (m), 1437 (M9), 1405 (m), 1346 (vs), 1318 (m), 1288 (m), 1254 (s), 1210 (m), 1176 (m), 1117 (m), 1034 (w), 965 (w), 854 (w), 832 (w), 811 (m), 791 (w), 748 (m), 593 (w), 495 (w), 431 cm⁻¹ (w); UV/Vis (CHCl₃): λ_{max} (*E_{rel}*)=526.1 (1.0), 489.5 (0.60), 459.0 nm (0.22); fluorescence (CHCl₃): λ_{max} =534, 575 nm; fluorescence quantum yield: (λ_{exc} =489 nm, *c*=7.2×10⁻⁶ mol L⁻¹ in chloroform, reference 2,9-bis-(1-hexylheptyl)anthra[2,1,9-*def*:6,5,10-*d'ef'*]diisoquinoline-1,3,8,10-tetraone^[4] with $\Phi=1.0$): 0.04; MS (70 eV): *m/z* (%): 708 (100) [*M*⁺], 691 (12) [*M*⁺-OH], 677 [*M*⁺-OMe], 527 (34) [*M*⁺-C₁₃H₂₅], 495 (78) [677-C₁₃H₂₆], 390 (14) [495-C₆H₂OMe], 373 (12) [390-OH], 345 (5) [373-CO]; elemental analysis calcd (%) for C₄₅H₄₄N₂O₆: C 76.25, H 6.26, N 3.95; found: C 76.10, H 6.28, N 3.89.

Compound PI-M4: 9-(1-Hexylheptyl)-2-benzopyrano[6',5',4':10,5,6]anthra[2,1,9-*def*]isoquinoline-1,3,8,10-tetraone (57 mg, 0.10 mmol) and 3,4-dimethoxyaniline (45 mg, 0.30 mmol) were allowed to react and the product was purified as was described for **PI-M3**. Yield: 50 mg (71%); m.p. >250°C; *R_f* (silica gel, CHCl₃/acetone 10:1)=0.71; ¹H NMR (300 MHz, CDCl₃): δ=0.76 (t, *J*(H,H)=6.6 Hz, 6H, 2×CH₃), 1.17–1.26 (m, 16H; 8×CH₂), 1.78–1.85 (m, 2H; α-CH₂), 2.15–2.22 (m, 2H; α-CH₂), 3.83 (s; -OCH₃), 3.89 (s; -OCH), 5.01–5.16 (m, 1H; -N-CH), 6.83–6.99 (m, 1H; CH_{aryl}), 7.19 (s, 1H; CH_{aryl}), 8.47–8.63 ppm (m, 8H; CH_{perylene}); ¹³C NMR (75 MHz, CDCl₃): δ=14.4 (CH₃), 23.0 (CH₂), 27.4 (CH₂), 29.6 (CH₂), 30.1 (CH₂), 32.2, (CH), 32.8, 55.3 (-OCH₃), 56.4 (-OCH₃), 56.5 (CH), 111.8, 112.2, 122.1, 123.4, 123.6, 126.6, 126.9, 128.1, 129.8, 130.0, 121.4, 132.0, 134.5, 135.3, 149.7, 150.1, 164.1 ppm; IR (KBr): $\tilde{\nu}$ =3436 (brm), 3078 (brw), 2956 (m), 2926 (m), 2856 (m), 1698 (s), 1660 (vs), 1595 (s), 1578 (m), 1514 (m), 1462 (w), 1433 (w), 1404 (m), 1346 (s), 1305 (w), 1254 (m), 1220 (w), 1176 (m), 1122 (m), 1028 (w), 966 (w), 860 (w), 810 (m), 794 (w), 746 (m), 619 (w), 490 (w), 431 cm⁻¹ (w); UV/Vis (CHCl₃): λ_{max} (*E_{rel}*)=526.7 (1), 490.2 (0.60), 459.0 nm (0.22); fluorescence (CHCl₃): λ_{max} =534, 576 nm; fluorescence quantum yield: (λ_{exc} =489 nm, *c*=7.0×10⁻⁶ mol L⁻¹ in chloroform, reference 2,9-bis-(1-hexylheptyl)anthra[2,1,9-*def*:6,5,10-*d'ef'*]diisoquinoline-1,3,8,10-tetraone^[4] with $\Phi=1.0$): 0.02; MS (70 eV): *m/z* (%): 708 (78) [*M*⁺], 691 (6), 526 (100) [*M*⁺-C₁₃H₂₆], 373 (36) [526-C₆H₂Me₂OH], 345 (5) [373-CO]; elemental analysis calcd (%) for C₄₅H₄₄N₂O₆: C 76.25, H 6.26, N 3.95; found C 76.50, H 6.14, N 3.94.

Compound PI-M5: 9-(1-Hexylheptyl)-2-benzopyrano[6',5',4':10,5,6]anthra[2,1,9-*def*]isoquinoline-1,3,8,10-tetraone (570 mg, 1.00 mmol) and 3,5-dimethoxyaniline (770 mg, 5.00 mmol) were allowed to react and the

product was purified as was described for **PI-M3**. Yield: 540 mg (76%); m.p. >250°C; R_f (silica gel, $\text{CHCl}_3/\text{acetone}$ 10:1)=0.81; $^1\text{H NMR}$ (300 MHz, CDCl_3): δ =0.85 (t, $J(\text{H,H})$ =6.6 Hz, 6H; $2\times\text{CH}_3$), 1.26–1.36 (m, 16H; $8\times\text{CH}_2$), 1.84–1.96 (m, 2H; $\alpha\text{-CH}_2$), 2.21–2.34 (m, 2H; $\alpha\text{-CH}_2$), 3.85 (s, 6H; $-\text{OCH}_3$), 5.16–5.26 (m, 1H; $-\text{NCH}$), 6.54 (d, $J(\text{H,H})$ =2.1 Hz, 2H; $\text{CH}_{\text{ortho-aryl}}$), 6.63 (t, 1H; $\text{CH}_{\text{para-aryl}}$), 8.63–8.76 ppm (m, 8H; $\text{CH}_{\text{perylene}}$); $^{13}\text{C NMR}$ (75 MHz, CDCl_3): δ =1.44 (CH_3), 23.0 (CH_2), 27.3 (CH_2), 29.6 (CH_2), 32.1 (CH_2), 32.8 (CH_2), 55.2 (CH), 55.9 ($-\text{OCH}_3$), 101.9, 107.2, 123.4, 123.7, 126.8, 127.1, 129.9, 130.2, 132.2, 134.7, 135.5, 137.1, 161.8, 163.8 ppm; IR (KBr): $\tilde{\nu}$ =3430 (brw), 3098 (brw), 2954 (m), 2927 (m), 2857 (m), 1770 (w); 1699 (s), 1662 (vs), 1594 (vs), 1578 (m), 1506 (m), 1465 (m), 1431 (m), 1405 (m), 1354 (vs), 1336 (s), 1322 (m), 1254 (m), 1218 (w), 1205 (m), 1176 (m); 1156 (m), 1127 (w), 1108 (w), 1063 (w), 966 (w), 926 (vw), 852 (w), 811 (m), 796 (w), 747 (m), 728 (w), 682 (w), 616 (vw), 590 (vw), 536 (vw), 496 (w), 431 cm^{-1} (w); UV/Vis (CHCl_3): λ_{max} (E_{rel})=526.8 (1), 489.8 (0.59), 458.9 (0.22) nm; fluorescence (CHCl_3): λ_{max} =533, 575 nm; fluorescence quantum yield (λ_{exc} =489 nm, $c=4.2\times 10^{-6}\text{ mol L}^{-1}$, reference 2,9-bis-(1-hexylheptyl)anthra[2,1,9-def;6,5,10-d'ef']diisoquinoline-1,3,8,10-tetraone^[4] with $\Phi=1.0$): 1.0; MS (70 eV): m/z (%): 708 (48) [M^+], 691 (6), 526 (100) [$M^+-\text{C}_{13}\text{H}_{26}$], 495 (2) [$527-\text{C}_{13}\text{H}_{26}\text{OMe}$], 391 (4), 373 (8) [$390-\text{OH}$]; elemental analysis calcd (%) for $\text{C}_{45}\text{H}_{44}\text{N}_2\text{O}_6$: C 76.25, H 6.26, N 3.95; found: C 76.56, H 6.32, N 3.86.

Compound PI-M7: 9-(1-Hexylheptyl)-2-benzopyrano[6',5',4':10,5,6]anthra[2,1,9-def]isoquinoline-1,3,8,10-tetraone (172 mg, 0.30 mmol) and 2,6-dimethoxyaniline (138 mg, 0.90 mmol) were allowed to react and the product was purified as was described for **PI-M3**. Yield: 210 mg (97%); m.p. >250°C; R_f (silica gel, $\text{CHCl}_3/\text{acetone}$ 10:1)=0.79; $^1\text{H NMR}$ (600 MHz, CDCl_3): δ =0.88 (t, $J(\text{H,H})$ =6.6 Hz, 6H; $2\times\text{CH}_3$), 1.28–1.39 (m, 16H; $8\times\text{CH}_2$), 1.90–1.94 (m, 2H; $\alpha\text{-CH}_2$), 2.27–2.33 (m, 2H; $\alpha\text{-CH}_2$), 3.84 (s; $-\text{OCH}_3$), 5.22–5.27 (m, 1H; N-CH), 6.78–6.79 (d, $J(\text{H,H})$ =8.4 Hz, 1H; CH_{aryl}), 7.31 (s, 1H; CH_{aryl}), 7.46–7.49 (t, 1H; CH_{aryl}), 8.73 ppm (dd, 8H; $\text{CH}_{\text{perylene}}$); $^{13}\text{C NMR}$ (150.9 MHz, CDCl_3): δ =14.4 (CH_3), 23.0 (CH_2), 27.4 (CH_2), 29.6 (CH_2), 32.2 (CH_2), 32.8 (CH_2), 55.2 (CH), 56.5 ($-\text{OCH}_3$), 104.9, 112.8, 123.4, 123.5, 126.9, 127.2, 130.0, 130.6, 130.8, 132.1, 135.2, 156.6, 163.2 ppm; IR (KBr): $\tilde{\nu}$ =3436 (brm), 2954 (m), 2927 (m), 2856 (w), 1714 (m), 1698 (s), 1658 (vs), 1595 (vs), 1579 (m), 1500 (w), 1481 (m), 1458 (w), 1434 (w), 1405 (m), 1344 (vs), 1307 (w), 1256 (m), 1200 (w), 1176 (w), 1140 (w), 1112 (m), 1034 (vw), 965 (w), 842 (w), 810 (m), 771 (w), 747 (m), 724 (w), 696 (vw), 614 (w), 494 (w), 432 cm^{-1} (w); UV/Vis (CHCl_3): λ_{max} (E_{rel})=526.1 (1), 489.2 (0.61), 458.2 nm (0.21); fluorescence (CHCl_3): λ_{max} =534, 575 nm; fluorescence quantum yield (λ_{exc} =489 nm, $c=4.2\times 10^{-6}\text{ mol L}^{-1}$ in chloroform, reference 2,9-bis-(1-hexylheptyl)anthra[2,1,9-def;6,5,10-d'ef']diisoquinoline-1,3,8,10-tetraone^[4] with $\Phi=1.0$): 1.0; MS (70 eV): m/z (%): 708 (100), [M^+], 691 (13) [$M^+-\text{OH}$], 623 (4), 539 (6), 527 (78) [$M^+-\text{C}_{13}\text{H}_{25}$], 495 (40) [$677-\text{C}_{13}\text{H}_{26}$], 465 (9) [$M^+-\text{OMe}$, $-\text{C}_{13}\text{H}_{28}$], 390 (67) [$495-\text{C}_6\text{H}_5\text{OMe}$], 373 (5) [$390-\text{OH}$], 345 (3) [$373-\text{CO}$]; elemental analysis calcd (%) for $\text{C}_{45}\text{H}_{44}\text{N}_2\text{O}_6$: C 76.25, H 6.26, N 3.95; found C 76.44, H 6.27, N 3.86.

Compound PI-M9: 9-(1-Hexylheptyl)-2-benzopyrano[6',5',4':10,5,6]anthra[2,1,9-def]isoquinoline-1,3,8,10-tetraone (980 mg, 1.7 mmol), 3,4,5-trimethoxyaniline (930 mg, 5.1 mmol), a catalytic amount of zinc acetate dihydrate, and imidazole (20 g) were heated at reflux (bath 130°C) for 4 h and then allowed to cool. While still warm, the solution was treated with 2N aqueous HCl (110 mL), collected by vacuum filtration, dried in air (120°C, 8 h), and purified by column separation (silica gel, chloroform/acetone 15:1). Yield: 1.12 g (84%); m.p. >250°C; R_f (silica gel/chloroform-acetone 15:1): 0.4; $^1\text{H NMR}$ (CDCl_3): δ =8.70 (d, $J(\text{H,H})$ =8 Hz, 2H; perylene), 8.65 (d, $J(\text{H,H})$ =8 Hz, 2H; perylene), 8.56 (d, $J(\text{H,H})$ =3 Hz, 2H; perylene), 8.53 (d, $J(\text{H,H})$ =3 Hz, 2H; perylene), 6.64 (s, 2H; phenyl), 5.21–5.16 (m, 1H; CH), 3.96 (s, 3H; phenyl), 3.90 (s, 6H; phenyl), 2.32–2.24 (m, 2H; CH_2), 1.96–1.88 (m, 2H; CH_2), 1.41–1.25 (m, 16H; CH_2), 0.86 ppm (t, $J(\text{H,H})$ =7 Hz, 6H, $2\times\text{CH}_3$); $^{13}\text{C NMR}$ (CDCl_3): δ =163.9 (C-O), 154.3, 138.6, 135.4, 134.4, 132.1, 132.1, 131.0, 130.0, 129.8, 126.9, 126.6, 123.6, 123.5, 123.4, 106.3, 61.3, 56.6, 55.3, 32.8, 32.2, 29.6, 27.4, 23.0, 14.4 ppm; IR (KBr): $\tilde{\nu}$ =3436 (s), 2928 (s), 2857 (m), 1699 (s), 1661 (s), 1595 (s), 1578 (w), 1506 (w), 1464 (w), 1433 (w), 1422 (w), 1405 (m), 1355 (m), 1328 (s), 1254 (m), 1176 (w), 1125 (m), 1008 (w), 965

(w), 853 (w), 810 (m), 796 (w), 747 (m), 723 (w), 677 (m), 498 (w), 431 cm^{-1} (w); UV (CHCl_3): λ_{max} (E_{rel})=527.6 (100), 490.9 (58.8), 459.8 nm (19.8); MS (70 eV): m/z (%): 738 (100) [M^+], 569 (2.51) [$M^+-\text{C}_9\text{H}_{11}\text{O}_3$], 556 (49.5) [$M^+-\text{C}_{13}\text{H}_{26}$]; elemental analysis calcd (%) for $\text{C}_{46}\text{H}_{46}\text{N}_2\text{O}_7$: C 74.82, H 6.46, N 3.73; found C 74.78, H 6.28, N 3.79.

Spectroscopy and photophysics: Spectrophotometric-grade toluene and dichloromethane (C. Erba) were used as supplied. Absorption spectra were measured in 10 mm cells using a Perkin-Elmer Lambda 950 UV/Vis spectrophotometer. A Spex Fluorolog II spectrofluorimeter was used to acquire fluorescence spectra from air-equilibrated solutions in 10 mm fluorescence cells. Experiments at 77 K made use of capillary tubes immersed in liquid nitrogen contained in a homemade quartz dewar. The reported luminescence spectra are uncorrected; emission quantum yields were determined after correction for the photomultiplier response, with reference to an air-equilibrated solution of N,N' -bis-(1-hexylheptyl)-3,4,9,10-perylenebis(dicarboximide) in dichloromethane with a $\Phi_{\text{fl}}=0.99$.^[5] Luminescence lifetimes in the nanosecond range were obtained using IBH single-photon counting equipment with excitation at 465 nm from pulsed diode sources (resolution 0.3 ns). The lifetimes in the picosecond range were measured using an apparatus based on a Nd:YAG laser (35 ps pulse duration, 532 nm, 1.5 mJ) and a Streak Camera Hamamatsu instrument. After deconvolution the resolution time is 5 ps. More details can be found elsewhere.^[23] Transient absorbances in the picosecond range were measured using a pump and probe system based on a Nd:YAG laser (Continuum PY62/10, 35 ps pulse, 532 nm, 3.5 mJ). Air-saturated solutions with an absorbance of 0.65 at 532 nm were employed. More details on the apparatus can be found elsewhere.^[24] Estimated errors are 10% on exponential lifetimes, 20% on quantum yields, 10% on molar-absorption coefficients, 2 nm on emission- and ground-state absorption peaks, and 10 nm in transient-absorbance peaks. If not otherwise specified, experiments were carried out at 295 K.

Molecular modeling: Fully optimized using the DFT B3LYP basis set 3-21G.

Acknowledgements

This work was supported by CIPS cluster, the Fonds der Chemischen Industrie, and by the CNR of Italy (PM.P04.010 MACOL).

- [1] See the following reviews and references therein: a) A. P. de Silva, T. S. Moody, G. D. Wright, *Analyst* **2009**, *134*, 2385–2393; b) T. Gunnlaugsson, M. Glynn, G. M. Tocci, P. E. Kruger, F. M. Pfeffer, *Coord. Chem. Rev.* **2006**, *250*, 3094–3117; c) C. W. Rogers, M. O. Wolf, *Coord. Chem. Rev.* **2002**, *233*, 341–350.
- [2] See the following reviews and references therein: a) A. Credi, *Angew. Chem.* **2007**, *119*, 5568–5572; *Angew. Chem. Int. Ed.* **2007**, *46*, 5472–5475; b) A. P. de Silva, S. Uchiyama, *Nat. Nanotechnol.* **2007**, *2*, 399–410; c) A. P. de Silva, T. P. Vance, M. E. S. West, G. D. Wright, *Org. Biomol. Chem.* **2008**, *6*, 2468–2481.
- [3] a) H. Langhals, *Helv. Chim. Acta* **2005**, *88*, 1309–1343; b) H. Langhals, *Heterocycles* **1995**, *40*, 477–500; c) H. Langhals, *Molecular Devices. Chiral Bichromophoric Silicones: Ordering Principles in Complex Molecules in Silicon Based Polymers* (Eds. F. Ganachaud, S. Boileau, B. Boury), Springer, Heidelberg, **2008**, pp. 51–63.
- [4] H. Langhals, J. Karolin, L. B.-Å. Johansson, *J. Chem. Soc. Faraday Trans.* **1998**, *94*, 2919–2922.
- [5] a) H. Langhals, A. J. Esterbauer, *Chem. Eur. J.* **2009**, *15*, 4793–4796; b) F. Würthner, *Chem. Commun.* **2004**, 1564–1579; c) F. Ilhan, D. S. Tyson, D. J. Stasko, K. Kirschbaum, M. A. Meador, *J. Am. Chem. Soc.* **2006**, *128*, 702–703; d) S. Vajravelu, L. Ramunas, G. J. Vidas, G. Valentas, J. Vyngintas, S. Valiaveetil, *J. Mater. Chem.* **2009**, *19*, 4268–4275; e) J. Fortage, M. Séverac, C. Houarner-Rassin, Y. Pellegrin, E. Blart, F. Odobel, *J. Photochem. Photobiol. A* **2008**, *197*, 156–169; f) H. Langhals, A. Obermeier, *Eur. J. Org. Chem.* **2008**,

- 6144–6151; g) H. Langhals, S. Poxleitner, O. Krotz, T. Pust, A. Walter, *Eur. J. Org. Chem.* **2008**, 4559–4562.
- [6] H. Langhals, A. Obermeier, Y. Floredo, A. Zanelli, L. Flamigni, *Chem. Eur. J.* **2009**, *15*, 12733–12744.
- [7] a) A. S. Lukas, Y. Zhao, S. E. Miller, M. R. Wasielewski, *J. Phys. Chem. B* **2002**, *106*, 1299–1306; b) F. Würthner, A. Sautter, D. Schmid, P. J. A. Weber, *Chem. Eur. J.* **2001**, *7*, 894–902; c) W. E. Ford, H. Hiratsuka, P. V. Kamat, *J. Phys. Chem.* **1989**, *93*, 6692–6696.
- [8] a) L. Flamigni, B. Ventura, M. Tasiar, T. Becherer, H. Langhals, D. T. Gryko, *Chem. Eur. J.* **2008**, *14*, 169–183; b) L. Flamigni, B. Ventura, C.-C. You, C. Hippius, F. Würthner, *J. Phys. Chem. C* **2007**, *111*, 622–630; c) A. I. Oliva, B. Ventura, F. Würthner, A. Camara-Campos, C. A. Hunter, P. Ballester, L. Flamigni, *Dalton Trans.* **2009**, 4023–4037; d) M. Tasiar, D. T. Gryko, J. Shen, K. M. Kadish, T. Becherer, H. Langhals, B. Ventura, L. Flamigni, *J. Phys. Chem. C* **2008**, *112*, 19699–19709.
- [9] a) S. Xiao, Y. Li, Y. Li, J. Zhuang, N. Wang, H. Liu, B. Ning, Y. Liu, F. Lu, L. Fan, C. Yang, Y. Li, D. Zhu, *J. Phys. Chem. B* **2004**, *108*, 16677–16685; b) W. Xu, H. Chen, Y. Wang, C. Zhao, X. Li, S. Wang, Y. Weng, *ChemPhysChem* **2008**, *9*, 1409–1415; c) B. Rybtchinski, L. E. Sinks, M. R. Wasielewski, *J. Am. Chem. Soc.* **2004**, *126*, 12268–12269; d) C. Flors, I. Oesterling, T. Schnitzler, E. Fron, G. Schweitzer, M. Sliwa, A. Herrmann, M. van der Auweraer, F. C. de Schryver, K. Müllen, J. Hofkens, *J. Phys. Chem. C* **2007**, *111*, 4861–4870; e) R. F. Kelley, W. S. Shin, B. Rybtchinski, L. E. Sinks, M. R. Wasielewski, *J. Am. Chem. Soc.* **2007**, *129*, 3173–3181; f) S. I. Yang, S. Prathapan, M. A. Miller, J. Seth, D. F. Bocian, J. S. Lindsey, D. Holten, *J. Phys. Chem. B* **2001**, *105*, 8249–8258; g) M. J. Arhens, R. F. Kelley, Z. E. X. Dance, M. R. Wasielewski, *Phys. Chem. Chem. Phys.* **2007**, *9*, 1469–1478; h) A. Prodi, C. Chiorboli, F. Scandola, E. Iengo, E. Alessio, R. Dobraza, F. Würthner, *J. Am. Chem. Soc.* **2005**, *127*, 1454–1462; i) F. J. Céspedes-Guirao, K. Ohkubo, S. Fukuzumi, A. Sastre-Santos, F. Fernández-Lázaro, *J. Org. Chem.* **2009**, *74*, 5871–5880; j) N. Van Anh, F. Schlosser, M. M. Groeneveld, I. H. M. van Stokkum, F. Würthner, R. Williams, *J. Phys. Chem. C* **2009**, *113*, 18358–18368.
- [10] H. Kaiser, J. Lindner, H. Langhals, *Chem. Ber.* **1991**, *124*, 529–535.
- [11] H. Langhals, *Chem. Ber.* **1985**, *118*, 4641–4645.
- [12] H. Langhals, S. Demmig, H. Huber, *Spectrochim. Acta* **1988**, *44A*, 1189–1193.
- [13] P. B. Merkel, P. Luo, J. P. Dinnocenzo, S. Farid, *J. Org. Chem.* **2009**, *74*, 5163–5173.
- [14] A. Zweig, W. G. Hodgson, W. H. Jura, *J. Am. Chem. Soc.* **1964**, *86*, 4124–4129.
- [15] M. Montalti, A. Credi, L. Prodi, M. T. Gandolfi, *Handbook of Photochemistry*, 3rd ed., CRC Press, Boca Raton, **2006**, pp. 624–627.
- [16] a) G. L. Gaines III, M. P. O’Neil, W. A. Svec, M. P. Niemczyk, M. R. Wasielewski, *J. Am. Chem. Soc.* **1991**, *113*, 719–721; b) L. Flamigni, E. Baranoff, J.-P. Collin, J.-P. Sauvage, *Chem. Eur. J.* **2006**, *12*, 6592–6606.
- [17] W. E. Ford, P. V. Kamat, *J. Phys. Chem.* **1987**, *91*, 6373–6380.
- [18] In this case, the CS-state energy level relative to the ground state, ΔG_{CS}^0 is calculated very simply from $\Delta G_{CS}^0 = E_{ox} - E_{red}$, without taking into account: 1) the Coulombic interaction and 2) the effect of the solvents on redox potentials used. There is a partial compensation of the two terms. The first is in fact a term that stabilizes the CS state, higher in low-dielectric constant media; the second is a destabilizing term, higher in low-dielectric media. The result is an overall increase of the CS-state energy level in TL compared to CH_2Cl_2 , that is, of a decrease of the driving force for charge separation and an increase of the driving force for charge recombination in TL relative to CH_2Cl_2 . Given the level of approximation involved in the present discussion, we consider the simplification acceptable and convenient.
- [19] R. A. Marcus, *Angew. Chem.* **1993**, *105*, 1161–1172; *Angew. Chem. Int. Ed. Engl.* **1993**, *32*, 1111–1121, and references therein.
- [20] P. O’Neill, S. Steenken, D. Schulte-Frohlinde, *J. Phys. Chem.* **1975**, *79*, 2773–2779.
- [21] a) J. Salbeck, H. Kumkely, H. Langhals, R. W. Saalfrank, J. Daub, *Chimia* **1989**, *43*, 6–9; b) T. Kircher, H. G. Löhmansröben, *Phys. Chem. Chem. Phys.* **1999**, *1*, 3987–3992.
- [22] A. A. Rachford, S. Goeb, F. N. Castellano, *J. Am. Chem. Soc.* **2008**, *130*, 2766–2767.
- [23] L. Flamigni, B. Ventura, A. I. Oliva, P. Ballester, *Chem. Eur. J.* **2008**, *14*, 4214–4224, and references therein.
- [24] L. Flamigni, A. M. Talarico, S. Serroni, F. Puntoriero, M. J. Gunter, M. R. Johnston, T. P. Jeynes, *Chem. Eur. J.* **2003**, *9*, 2649–2659, and references therein.

Received: May 28, 2010
Published online: October 7, 2010